Evidence for Two Concentration-Dependent Processes for β-Subunit Effects on α1B Calcium Channels

C. Cantí, A. Davies, N. S. Berrow, A. J. Butcher, K. M. Page, and A. C. Dolphin
Department of Pharmacology, University College London, London WC1E 6BT, United Kingdom

ABSTRACT β-Subunits of voltage-dependent Ca^{2+} channels regulate both their expression and biophysical properties. We have injected a range of concentrations of β3-cDNA into *Xenopus* oocytes, with a fixed concentration of α1B ($Ca_V2.2$) cDNA, and have quantified the corresponding linear increase of β3 protein. The concentration dependence of a number of β3-dependent processes has been studied. First, the dependence of the a1B maximum conductance on β3-protein occurs with a midpoint around the endogenous concentration of β3 (~17 nM). This may represent the interaction of the β-subunit, responsible for trafficking, with the I-II linker of the nascent channel. Second, the effect of β3-subunits on the voltage dependence of steady-state inactivation provides evidence for two channel populations, interpreted as representing α1B without or with a β3-subunit, bound with a lower affinity of 120 nM. Third, the effect of β3 on the facilitation rate of G-protein-modulated α1B currents during a depolarizing prepulse to +100 mV provides evidence for the same two populations, with the rapid facilitation rate being attributed to Gβγ dissociation from the β-subunit-bound α1B channels. The data are discussed in terms of two hypotheses, either binding of two β-subunits to the α1B channel or a state-dependent alteration in affinity of the channel for the β-subunit.

INTRODUCTION

Voltage-dependent Ca^{2+} channels (VDCCs) are composed of a pore-forming α1-subunit, associated with accessory subunits, including a cytoplasmic β-subunit and largely extracellular α2δ-subunit (Dolphin, 1998, for review). β-Subunits regulate a number of properties of VDCCs, increasing current density, in part by recruitment of channels into the plasma membrane (Brice et al., 1997; Bichet et al., 2000) and hyperpolarizing the voltage dependence of activation and also steady-state inactivation (except in the case of β2a) (De Waard and Campbell, 1995; Stephens et al., 1997). A role for β-subunits in G-protein inhibition of calcium channels has also been reported (Campbell et al., 1995; Bourinet et al., 1996; Qin et al., 1997; Roche and Treistman, 1998; Meir et al., 2000). This has been interpreted in terms of an interaction at an overlapping binding site (Bourinet et al., 1996). However, we have shown that there is not a simple competition between β-subunits and Gβγ dimers (Meir et al., 2000; Canti et al., 2000). Indeed, in a system (COS-7 cells) in which no endogenous β-subunit protein was detected by immunocytochemistry, the presence of heterologously expressed β-subunits was essential for the relief of Gβγ-mediated inhibition by prepulse facilitation (Meir et al., 2000).

The point has recently been made that we do not know how many β-subunits bind physiologically to a functional calcium channel (Birnbaumer et al., 1998). Three Gβγ and β-subunit interaction sites have been identified on various α1-subunits, and a high-affinity site within the I-II loop (Zamponi et al., 1997; De Waard et al., 1997) and other interaction sites of lower affinity were measured on the C terminus (Qin et al., 1997; Walker et al., 1998) and the N terminus (Walker et al., 1999; Canti et al., 1999; Stephens et al., 2000). However, none of these studies has been able to address whether in an intact channel the same β-subunit binds with high affinity to the I-II linker and interacts via different domains with lower affinity at the N and C termini. It is certainly possible that these three intracellular domains of α1-subunits all form part of a complex binding pocket for both a single β-subunit and, when present, a Gβγ dimer. Alternatively, several β-subunits might bind to different sites on the same channel.

The aim of the present work was to examine the dependence of a number of the effects of VDCC β-subunits on the concentration of β3-subunit expressed in *Xenopus* oocytes. We wished to determine whether we could distinguish different concentration dependencies, which would provide evidence for more than one binding process for β-subunits. We have examined the effect of β3-subunit concentration on the maximum conductance of α1B, as a measure of expression level, on the voltage dependence of steady-state inactivation, and on the rate of prepulse facilitation during G protein inhibition. We have not examined the effects of β3 on inactivation kinetics, because in a previous study, we found little effect of β3 on this parameter for α1B (Stephens et al., 2000).

MATERIALS AND METHODS

Expression of constructs

The following cDNAs were used: rabbit α1B (GenBank L15453) and the I49A mutant of α1B (Canti et al., 2000), rat β3 (M88751), rat α2δ-1 (M86621), and rat $D2_{long}$ dopamine receptor (X17458, N5→G) in the vector pMT2. *Xenopus* oocytes were prepared, injected, and maintained as

Received for publication 5 March 2001 and in final form 12 June 2001.

Address reprint requests to Dr. A. C. Dolphin, Department of Pharmacology, University College London, Gower Street, London WC1E 6BT, UK. Tel.: 44-20-7679-3054; Fax: 44-20-7813-2808; E-mail: a.dolphin@ucl.ac.uk.

0006-3495/01/09/1439/13 $2.00

described previously (Canti et al., 2000). The α1B, β3, α2δ-1, and D2 receptor cDNAs (1 ng nl^{-1}, except for the β-subunit) were mixed in a ratio of 3:4:1:3, respectively, and 4 nl was injected (except when otherwise stated) into the nuclei of stage V and VI oocytes. The β3 cDNA was diluted up to 1:500 before mixing, and when β3 cDNA was not used, it was replaced by buffer. The entire range of β3 cDNA concentrations was examined in each experiment to minimize batch-to-batch variation in oocyte expression levels.

Antisense oligonucleotides

The 25-mer antisense oligonucleotide DNA (ODN) sequence used was **GCA** CTC CTC ATC CAG CGC TCC A**CA G** (Tareilus et al., 1997). The scrambled nonsense ODN sequence was **CTC** GTA GCG CAC CAC CTA CCT C**AG C** (Gibco, Paisley, UK). The nucleotides were phosphodiester linked, except the first and last three nucleotides, in bold, which were phosphorothioate linked, to reduce degradation. In these experiments α1B cDNA, α2δ-1 cDNA, and ODN (4 or 40 μM) were mixed in a ratio of 3:1:3 before injection of 9 nl per oocyte.

Expression and purification of H6Cβ3

A full-length β3 with C-terminal hexahistidine tag (H6Cβ3) was produced by two-stage polymerase chain reaction (PCR) to remove an internal *Afl*III site (10 cycles each stage) using *Pfu* polymerase (Stratagene, Amsterdam, The Netherlands), β3 in pMT2 as template, and the following primers for stage one: forward, 5′CCCACATGTATGACGACTCC3′; reverse, 5′CGGGGGGACATGCTCCGCCTGCTTTT3′.

The resulting PCR product was purified and used as the forward primer in the second stage reaction with 5′GGGAATTCTCAATGATGATGAT-GATGATGGTAGCTGTCCTTAGGCCA3′ as the reverse primer. The resulting PCR product (~1.5 kb) was purified from agarose gel, digested with *Afl*III and *Eco*RI, and sub-cloned into *Nco*I- and *Eco*RI-digested pET28b (Novagen, Nottingham, UK) to give H6Cβ3-pET28b. BL21 Codon Plus (IRL) *Escherichia coli* (Stratagene) were transformed with H6Cβ3-pET28b, and cultures were grown overnight to saturation at 37°C in LB (pH 5.5) supplemented with kanamycin, chloramphenicol, and 1% w/v glucose, diluted 1:10 with the same medium, and grown for an additional 3 h before cooling to room temperature and induction with 0.5 mM isopropylthio-β-D-galactoside. The cultures were grown for 3 h after induction and harvested by centrifugation; pellets were then stored at −70°C until required.

E. coli pellets containing expressed H6Cβ3 protein were lysed at 4°C by sonication in 20 mM phosphate buffer (pH 7.4), containing one protease inhibitor tablet (Complete EDTA-free, Roche Diagnostics, Lewes, UK) per liter of pelleted culture. Solid NaCl was added to the lysate to a final concentration of 1 M NaCl before the lysate was cleared at 20,000 × *g* at 4°C for 15 min. Imidazole solution (pH 7.4) was then added to the resulting supernatant to give a final concentration of 20 mM before loading onto a Ni^{2+}-primed 5-ml HiTrap chelating column (Amersham Pharmacia, Uppsala, Sweden) equilibrated with load buffer (20 mM phosphate buffer, pH 7.4, 1 M NaCl, 20 mM imidazole, 0.15% w/v octylglucoside, and one protease inhibitor tablet per 100 ml). The column was washed thoroughly with wash buffer (same as load buffer but with 40 mM imidazole) before H6Cβ3 was eluted from the column in elution buffer (same as load buffer but with 200 mM imidazole).

Peak UV_{280} absorbance fractions were rapidly buffer exchanged on a Sephadex G-25 (Amersham Pharmacia) column into ion-exchange (IEX) buffer (20 mM 2-[*N*-morpholino] ethanesulfonic acid, pH 6.0, one protease inhibitor tablet per 200 ml) supplemented with 500 mM NaCl, before dilution 1:10 with IEX buffer. The diluted sample was loaded onto a 1-ml SP-Sepharose HP column (Pharmacia), and the column was washed with IEX buffer before H6Cβ3 proteins were eluted in a linear gradient of 0–1 M NaCl in IEX buffer. Fractions containing H6Cβ3 were identified by sodium dodecyl sulfate-polyacrylamide gel electrophoresis (SDS-PAGE) analysis, with Coomassie blue staining, before concentrating to 0.5 mg ml^{-1} using Centriplus concentrators.

Surface plasmon resonance binding assay

All assays were performed on a Biacore 2000 (Biacore, Uppsala, Sweden) at 25°C in 10 mM Hepes, 500 mM NaCl, 3 mM EDTA, 0.005% polysorbate-20, pH 7.4. Glutathione S-transferase (GST) and the GSTα_{1B}I-II linker fusion proteins were purified as previously described (Bell et al., 2001) and immobilized on individual flow cells of a CM5 dextran chip using an anti-GST polyclonal antibody kit (Biacore) according to the manufacturer's instructions. To obtain identical molar loadings of the different molecular mass proteins the following resonance unit (RU) correction factors were used during immobilization: GST = 1; GSTα_{1B}I-II linker = 1.57. H6Cβ3 protein was diluted as stated, and H6Cβ3 injections were performed using a flow rate of 50 μl min^{-1} for 5 min.

Determination of the amount of β3-subunit in *Xenopus* oocytes

Oocytes were injected intranuclearly, as described previously (Canti et al., 2000), with α1B/α2δ-1 subunits and either 3, 45, 720, or 1440 pg of β3 cDNA. After 5 days of incubation at 18°C, individual oocytes (following brief electrophysiological recording to verify expression of α1B I_{Ba}) were lysed in hypotonic buffer (10 mM Tris, pH 7.4, containing protease inhibitors (Roche) plus 1 mM EDTA), solubilized in 2% SDS, assayed for protein content, diluted as necessary to remain within the linear range (see Fig. 2), and separated by SDS-PAGE, followed by immunoblotting for β3-subunits. H6Cβ3 subunit standards (0.2–3 ng) were run in parallel. The polyvinylidene fluoride membranes were blocked with 3% bovine serum albumin for 5 h at 55°C and incubated overnight at 20°C with a 1:500 dilution of anti-β3 monoclonal antibody raised against residues 418–484 of human β3 (Day et al., 1998; Bogdanov et al., 2000). This region is 97% and 80% identical to the corresponding rat and *Xenopus* β3 sequence, respectively. Because the antibody is a monoclonal, it is highly likely to bind to an epitope that is well conserved between the three species. The primary antibody was followed by a 1:1000 dilution of goat anti-mouse IgG-horseradish peroxidase conjugate (BioRad Laboratories, Richmond, CA) for 1 h at 20°C. Detection was performed using ECL (Amersham Pharmacia Biotech), the films were subsequently scanned, and the amount of β3 subunit in each sample was determined using Imagequant (Molecular Dynamics, Sunnyvale, CA) from the standard curve of purified H6Cβ3 protein on the same blots. To estimate the β-subunit content of plasma membrane and internal (cytosolic) fractions, oocytes were placed in hypotonic buffer (5 mM Hepes, pH 7.4, with protease inhibitors) for 30 min at room temperature. The plasma membrane was then isolated with fine forceps from the cell interior contents (cytosol). The two fractions from a given number of oocytes were pooled and each homogenized in hypotonic buffer. The plasma membrane fractions were washed three times in hypotonic buffer by centrifugation (100,000 × *g* for 30 min at 4°C). Both fractions were solubilized in SDS-PAGE buffer and then assayed for β3 and total protein content.

Electrophysiological recording of I_{Ba}

Two-electrode voltage-clamp recordings from oocytes were performed as described previously (Canti et al., 2000). Oocytes were held at −100 mV, and currents were evoked every 15 s using 5 mM Ba^{2+} as charge carrier, unless otherwise stated. The α1B I_{Ba} was always recorded using the same sequence and timing of protocols. For every cell, a maximal concentration of quinpirole (100 nM) was applied, after which marked and prolonged over-recovery (>30 min) was usually observed due to the removal of tonic

inhibition (Canti et al., 2000). This provided a stable baseline from which all experimental measurements were then made. All experimental data regarding the effect of quinpirole application were obtained during a second application of the drug. Current amplitude measurements were taken at 20 ms after the start of test pulses except in the steady-state inactivation protocol, where currents were measured at their peak. All values are mean ± SEM, and statistical significances were determined by Student's *t*-test.

The observed α1B I_{Ba} currents were not contaminated with endogenous oocyte currents, as these were measured in non-injected oocytes from every batch and were less than 10 nA for the maximum I_{Ba} in 5–10 mM Ba^{2+}. All currents were leak-subtracted on-line using a −P/4 protocol.

Data analysis

Data were analyzed using Clampfit (Axon Instruments, Foster City, CA) and ORIGIN 5.0 (Microcal, Northampton, MA).

Current-voltage (*IV*) curves were fit to a combined Boltzmann and linear function:

$$I = G_{max}(V_t - V_{rev})/[1 + \exp(-(V_t - V_{50,act})/k)],$$

where V_t represents the test potential, G_{max} the maximum conductance, V_{rev} the apparent reversal potential, $V_{50,act}$ the potential for half-activation, and k the slope factor.

The steady-state inactivation curves were either fit by a single Boltzmann function:

$$I/I_{max} = 1/[1 + \exp((V_t - V_{50,inact})/k)],$$

where I_{max} is the peak current value, $V_{50,inact}$ is the potential for half-inactivation, or to a double Boltzmann function:

$$I/I_{max} = 1 - (a/[1 + \exp((V_t - V_{50,inact,a})/k_a)] - b/[1 + \exp((V_t - V_{50,inact,b})/k_b)]),$$

where $V_{50,inact,a}$ and k_a are the parameters associated with the component A of amplitude a, and $V_{50,inact,b}$ and k_b are the corresponding parameters associated with the second component B of amplitude $b = (1 - a)$. The χ^2 values associated with each fit were used to assess whether a single or double function best fit each individual dataset.

RESULTS

To examine how the biophysical effects of β-subunits are dependent on expressed β-subunit concentration, we have expressed a range of concentrations of the VDCC β3-subunit by injecting increasing amounts of β3 cDNA, from 0 to 720 pg, together with a fixed concentration of α1B and α2δ-1 cDNA into *Xenopus* oocytes. The rat β3-subunit was used because it is one of the main β-subunits associated with α1B in native tissues (Witcher et al., 1993; Burgess et al., 1999). Furthermore, using a PCR strategy with primers in regions of homology between all mammalian β-subunits, only β3 cDNA was isolated from *Xenopus* oocytes, and it is therefore reasonable to conclude that it is the only β-subunit present in these cells (Tareilus et al., 1997). In agreement with this, comparison of results obtained with the β3 antibody used in this study, and a pan-β-subunit antibody (Campbell et al., 1995), revealed no additional β-subunit immunoreactive bands on immunoblots (results not shown).

Determination of the endogenous β3-subunit concentration in *Xenopus* oocytes and that resulting from injection of increasing β3 cDNA

The relationship between the concentration of β3 cDNA injected into the *Xenopus* oocytes and the amount of β3 protein expressed was examined by constructing a standard curve with H6Cβ3 (Fig. 1 *a*) and using this to determine the amount of β3 protein in non-injected and β3 cDNA-injected oocytes. The expression of β3 protein was linear up to the highest amount of injected β3 cDNA examined (1.44 ng), which is twice the maximum amount used in the electrophysiological experiments (Fig. 1 *b*). The endogenous β3 level in α1B/α2δ-1-injected oocytes was very similar to that in non-injected oocytes (112 ± 2% of the non-injected level; $n = 10$). Furthermore, it was reduced by 47 ± 4% ($n = 10$) after 40 μM A/S ODN injection (Fig. 1 *b*). The amount of endogenous β3 per oocyte was 0.56 ± 0.02 ng ($n = 15$), which corresponds to an average concentration of ~17 nM, assuming an oocyte radius of 0.5 mm. The ratio of β3 protein associated with the plasma membrane and internal fraction was examined at the different concentrations of β3 cDNA injected into *Xenopus* oocytes (Fig. 1 *c*). Although the amount of β3-subunit was linearly dependent on β3 cDNA concentration in both fractions (Fig. 1 *c*, *inset*), that in the internal (cytosolic) fraction increased to a much greater extent, as expected, because β3 is unlikely to be plasma membrane associated unless bound to a calcium channel (Bogdanov et al., 2000). The ratio (per oocyte) of β3 protein in the cytosol/membrane rises to over 30 at the highest concentration of β3 cDNA used.

Dependence of the α1B G_{max} on the concentration of β3-subunit resulting from co-expression of increasing amounts of β3 cDNA

We first examined the influence of increasing the β3-subunit concentration on the G_{max} obtained from the α1B *IV* relationships (Fig. 2). Examples of I_{Ba} at 0 mV are shown in Fig. 2 *a*, *i*, and the mean *IV* relationships in Fig. 2 *b*. In the absence of expressed β3-subunit, the G_{max} was 0.014 ± 0.002 μS ($n = 13$). The G_{max} showed strong dependence on the expressed β3-subunit, with 15 pg of injected β3 cDNA giving a plateau G_{max} of 0.029 ± 0.004 μS ($n = 19$). The $V_{50,act}$ showed a more gradual hyperpolarizing shift with increasing β3-subunit to a maximum of −15.3 mV (see Fig. 2 *e*), resulting in an increased current amplitude at 0 mV, after the conductance increase had saturated, because of the increased driving force at the more hyperpolarized potentials (Fig. 2, *a* and *b*). There was no effect of β3-subunit expression on the V_{rev} (see Fig. 2).

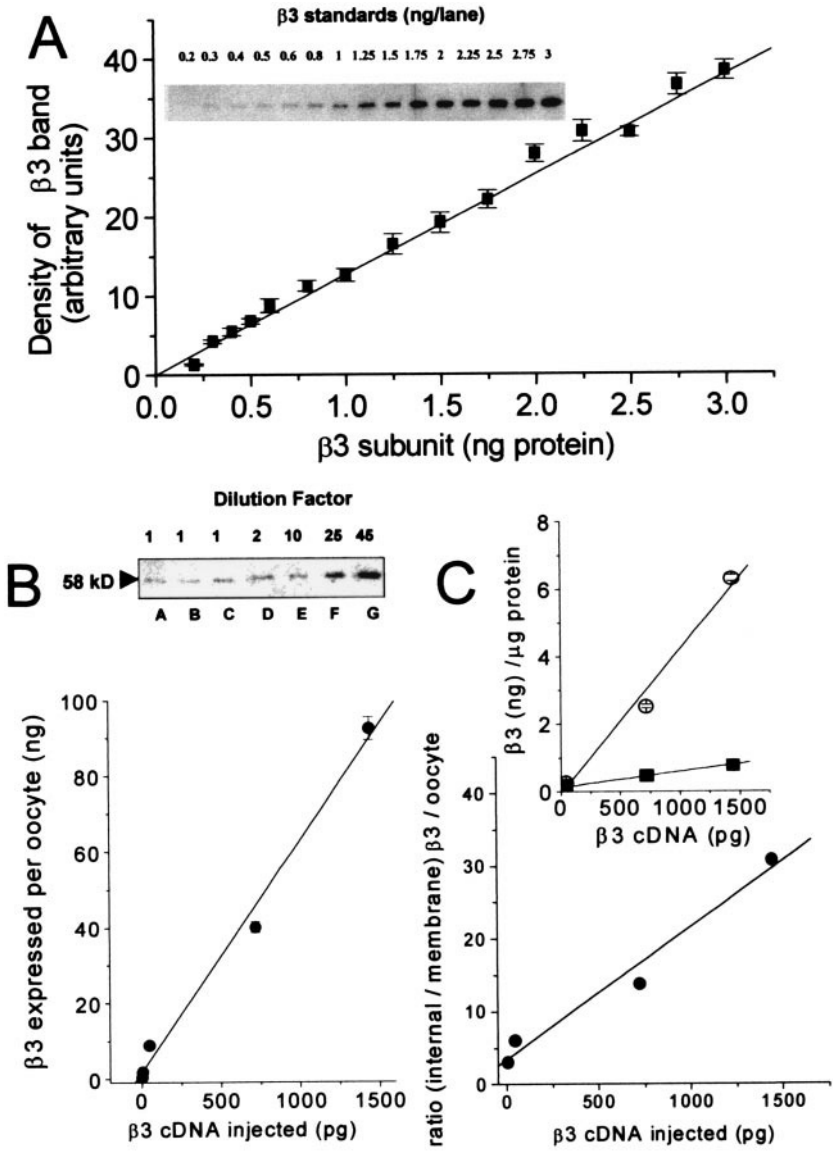

FIGURE 1 Dependence of *Xenopus* oocyte $\beta 3$ protein level on $\beta 3$ cDNA injected. (*a*) Standard curve for $\beta 3$ protein from 0.2–3 ng (mean ± SEM; $n = 5$). H6C$\beta 3$ was purified and detected using a $\beta 3$ monoclonal antibody as described. The same protein band was also detected with an anti-hexahistidine antibody (results not shown). The straight line is a linear regression fit ($y = 12.6x$; $R = 0.993$), from which the amount of $\beta 3$ in oocyte lysates was determined. The inset at the top shows a representative immunoblot of the standard curve, using the H6C$\beta 3$ protein whose purity is shown in Fig. 3 *a*. (*b*) Immunodetection of $\beta 3$ subunits in total oocyte lysates using the $\beta 3$ monoclonal antibody. (*Inset*) Representative immunoblot. Oocytes were injected as follows: lane A, no injected DNA; lane B, $\alpha 1B/\alpha 2\delta$-1 + A/S ODN 40 μM; lane C, $\alpha 1B/\alpha 2\delta$-1 alone; lanes D—G, $\alpha 1B/\alpha 2\delta$-1 + 3 pg, 45 pg, 720 pg, and 1.44 ng of $\beta 3$ cDNA, respectively. The dilutions used are indicated above the blots. For the graph, the total optical density of the $\beta 3$ bands was determined and the $\beta 3$ level calculated from the standard curve and plotted against $\beta 3$ cDNA injected (●). Data are mean ± SEM of 10–15 values each. The line is a linear regression fit to the data ($y = 1.79 + 0.061x$; $R = 0.995$). (*c*) $\beta 3$ subunits were quantified by immunodetection in isolated oocyte plasma membrane and internal protein fractions using the $\beta 3$ monoclonal antibody. The ratio of $\beta 3$ subunit/oocyte in the internal/oocyte membrane fraction is shown as a function of increasing amounts of injected $\beta 3$ cDNA (3, 45, 720, and 1440 pg; ●) in addition to $\alpha 1B$ and $\alpha 2\delta$-1 subunits. Data are the ratio of mean values for of 8–20 determinations each. The line is the linear regression fit to the data ($R = 0.987$). The inset plot shows separately the increase in $\beta 3$ subunit in the internal (○) and oocyte membrane fractions (■) from which the ratios were determined.

Effect of a $\beta 3$ antisense ODN on $\alpha 1B$ calcium channel expression in *Xenopus* oocytes

To determine to what extent the expression of $\alpha 1B$ currents, in the absence of co-expressed β subunits, relies on the presence of the endogenous *Xenopus* oocyte β-subunits, a $\beta 3$ A/S ODN was injected, together with $\alpha 2\delta$-1 cDNA and a higher concentration of $\alpha 1B$ cDNA (see Materials and Methods). A scrambled N/S ODN was used as a control. Two different A/S ODN concentrations were used (4 and 40

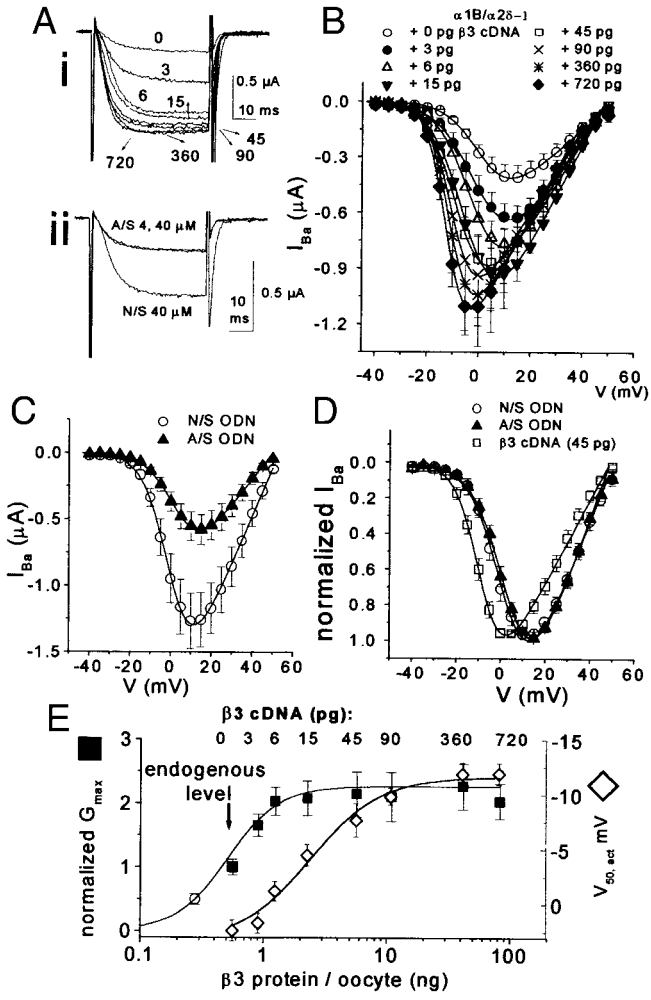

FIGURE 2 Modulation of α1B biophysical properties by co-expression of VDCC β subunits or β3 antisense ODNs. The α1B channel was expressed with α2δ-1 and the dopamine D2 receptor and either without or with 3–720 pg of β3 cDNA or with A/S or N/S ODNs. (*a*) Example currents at 0 mV: (*i*) for the different concentrations of β3 cDNA as given; (*ii*) for A/S ODN (4 and 40 μM), compared with N/S ODN (40 μM). (*b*) *IV* relationships for the different concentrations of β3 cDNA (symbols given in key) were obtained from voltage steps between −40 and +50 mV, and I_{Ba} at 20 ms was fit to a modified Boltzmann function (see Materials and Methods). The $V_{50,act}$ values were (mV) 2.8 ± 0.9 (0 pg of β3 cDNA, n = 13); 1.4 ± 1.6 (3 pg, n = 13); −1.2 ± 0.9 (6 pg, n = 19); −4.3 ± 0.9 (15 pg, n = 19); −8.5 ± 1.0 (45 pg, n = 10); −9.8 ± 0.8 (90 pg, n = 12); −11.9 ± 1.0 (360 pg, n = 9), and −12.5 ± 0.9 (720 pg, n = 9). The k (slope factor) values were between 3.8 and 5.7 mV. The V_{rev} values in all groups lay between 44.3 mV and 50.3 mV, with no statistically significant differences between them and no effect of β3 subunit co-expression. (*c*) *IV* relationships comparing the A/S and N/S conditions: ○, 40 μM N/S ODN, n = 9; ▲, mean of 4 and 40 μM A/S ODN, n = 8. (*d*) Normalized *IV* relationships for the N/S and A/S ODN conditions (same symbols as in *c*), showing the lack of effect on the $V_{50,act}$. In comparison, the normalized *IV* relationship for the 45 pg of β3 cDNA condition is also given (□, n = 10). (*e*) The G_{max} was determined as the slope conductance from the linear region of the *IV* relationships, normalized to the value for α1B/α2δ-1 and plotted against the amount of β3 protein calculated from the linear regression fit to Fig. 1 *b* (*left axis*, ■). The open circle represents the G_{max} determined following the A/S ODN relative to the N/S ODN data from *c*. The data are fit by a logistic function with a midpoint of 0.54 ng of β3 protein and a power coefficient of 1.9. The arrow represents the measured endogenous β3 protein level. The amount of β3 cDNA injected is indicated above each point. The $V_{50,act}$ values were determined from the *IV* relationships in *b* and are plotted against the amount of β3 protein (*right axis*, ◇). The data are fit by a logistic function with a midpoint of 2.71 ng of β3 protein and a power coefficient of 1.7.

μM), which gave very similar results. For the oocytes injected with the N/S ODN, 11/12 oocytes expressed I_{Ba} (Fig. 2 *a*, *ii*), and from the *IV* relationship (Fig. 2 *c*) the G_{max} was 0.036 ± 0.006 μS (n = 9). For 4 and 40 μM β3 A/S ODN, 5/15 and 5/20 oocytes, respectively, expressed I_{Ba} above background noise (Fig. 2 *a*, *ii*), and from these oocytes the G_{max} was 0.018 ± 0.004 μS (n = 4) and 0.019 ± 0.007 μS (n = 4), respectively (see Fig. 2 *c* for a comparison of the N/S and pooled A/S data). It is clear from the normalized *IV* relationships that although the β3 A/S ODN reduced G_{max} by ~50%, it did not significantly depolarize the $V_{50,act}$ compared with either the N/S ODN (Fig. 2 *d*) or the 0-pg β3 cDNA control. The $V_{50,act}$ was +2.8 ± 0.9 mV for α1B/α2δ-1 (n = 13), +1.4 ± 1.7 mV for α1B/α2δ-1 + 40 μM N/S ODN (n = 9), +2.5 ± 2.1 mV for α1B/α2δ-1 + 4 μM A/S ODN (n = 4), and +4.5 ± 0.7 mV for α1B/α2δ-1 + 40 μM A/S ODN (n = 4). In comparison, 45 pg of β3 cDNA, a concentration that produced an approximate doubling of the G_{max} compared with the α1B/α2δ-1 control (Fig. 2 *b*) and an ~10-fold increase in β3 protein (Fig. 1 *b*), also caused a marked hyperpolarizing shift in the $V_{50,act}$ to −8.5 ± 1.0 mV (n = 10; Fig. 2*d*).

By estimating the β3 protein level for each β3 cDNA concentration used, from linear regression of the data in Fig. 1 *b* and taking into account the dilution factor used, we then determined the dependence of α1B G_{max} on amount of β3 protein expressed per oocyte (Fig. 2 *e*, ■). The data, including the point generated from the A/S experiment (○), are well fit by a sigmoid concentration-response curve. The midpoint of this curve (0.54 ng of β3 protein per oocyte, approximately equivalent to 16.3 nM) occurs at about the endogenous level of β3 protein in the *Xenopus* oocytes, and the plateau is reached at ~2.3 ng of β3 protein per oocyte (69 nM).

We also examined the concentration dependence of the $V_{50,act}$ (Fig. 2 *e*, ◇) and found it to be fit by a sigmoid concentration-response curve with a higher midpoint at 2.7 ng of β3 protein.

Binding affinity of the purified β3 protein for the I-II linker of α1B

The same purified H6Cβ3 protein used for the quantification of endogenous and expressed β3 levels (Fig. 3 *a*) was also used to examine its binding to the α1B I-II linker immobilized as a GST fusion protein (Fig. 3 *a*) on a Biacore

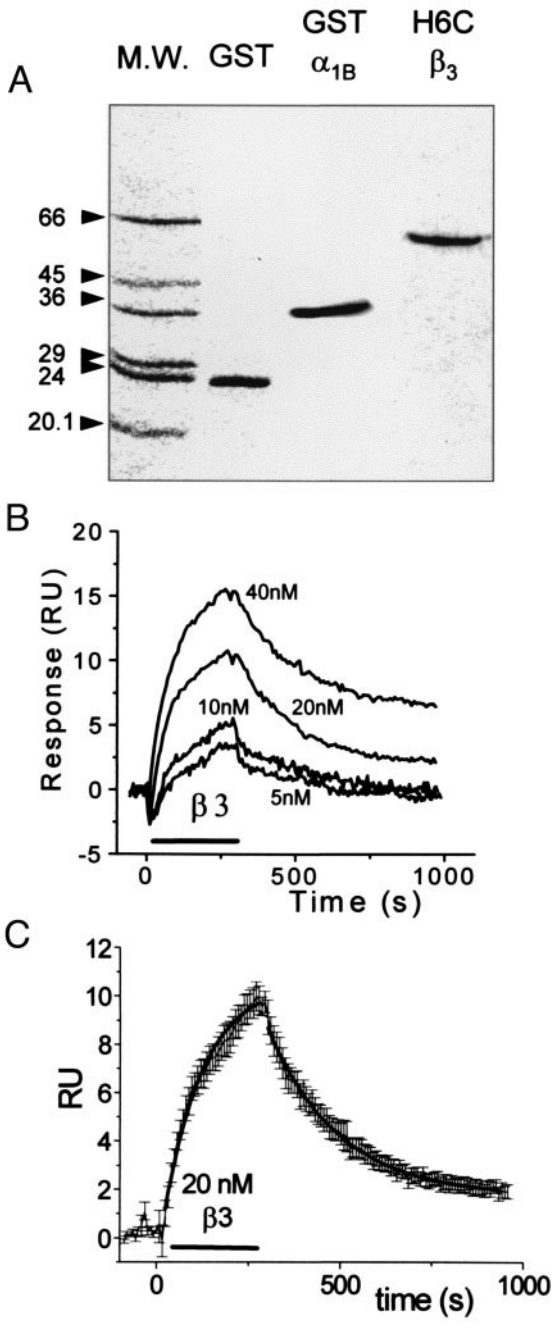

FIGURE 3 Binding of β3 protein to GST fusion proteins of α1B I-II linker. (*a*) Coomassie-blue-stained 12.5% SDS-PAGE gel (Brabet et al., 1988) of the proteins used in the surface plasmon resonance binding assay. Approximately 0.5 μg of the following proteins was loaded: GST, GSTα_{1B}I-II loop, and H6Cβ3. The positions of molecular mass markers (Sigma) are shown for comparison. (*b*) Examples of Biacore 2000 sensorgrams. Approximately 4 fmol of the fusion protein or GST was immobilized via the anti-GST antibody on an individual flow cell of a CM5 dextran sensor chip. The VDCC β3 protein was diluted to the concentrations stated (5, 10, 20, and 40 nM β3) and injected over all flow cells at a flow rate of 50 μl min^{-1} for 5 min. The resulting sensorgram from the flow cell containing GST was subtracted from those containing the GSTα_{1B}I-II loop as a correction for bulk refractive index changes during β3 perfusion and for nonspecific binding of the β3 analyte to the GST moieties of the fusion protein. (*c*) Mean sensorgram for 20 nM β3 subunit. The data are the mean ± SEM of six separate experiments. The single-exponential fits to the on- and off-rates of the mean sensorgram are shown in bold lines (τ_{on} = 107 s, and τ_{off} = 190.7 s). Assuming 1:1 binding, the K_D was obtained from k_{off}/k_{on}, where k_{off} is determined directly from τ_{off}, and k_{on} is calculated from $(1/\tau_{on}) = k_{on} \times [\beta] + k_{off}$. From the mean data, k_{off} was 5.2 × 10^{-3} s^{-1}. However, this may be an underestimate as the k_{off} derived from Biacore data may be contaminated by rebinding of the ligand. The calculated k_{on} was 2.0 × 10^5 M^{-1} s^{-1}.

2000. The binding of H6Cβ3 was concentration dependent and reversible, between 5 and 40 nM H6Cβ3, the highest concentration examined (n = 3–6 for each concentration; example sensorgrams given in Fig. 3 *b*). The mean sensorgram for 20 nM H6Cβ3 is shown in Fig. 3 *c* (n = 6). Both the on- and off-rates were well fit by a single-exponential function to the mean data, and the K_D was determined to be 26 nM (see legend to Fig. 3 *c*). Similarly, for the 10 nM β3 binding data, the mean K_D was calculated to be 19.6 nM, from fits of the on- and off-rates for the mean data (n = 3; results not shown). These estimates of the affinity of H6Cβ3 binding to the α1B I-II linker are in very good agreement with the functional data. The specific k_{on} for H6Cβ3 binding to the α1B I-II linker in this system was estimated to be 2.0 × 10^5 M^{-1} s^{-1} (see Fig. 3 *c*).

Dependence of steady-state inactivation of α1B on the concentration of β3-subunit resulting from co-expression of increasing amounts of β3 cDNA

We next examined the effect of heterologous expression of the β3-subunit on the steady-state inactivation of α1B currents. For the two extreme conditions, no β3 cDNA (and therefore no heterologously expressed β3-subunit) and the maximal amount (720 pg) of β3 cDNA injected, the data could be fit by a single Boltzmann function (Fig. 4 *a*). The $V_{50,inact}$ was hyperpolarized by the co-injection of 720 pg of β3 cDNA from −38.7 ± 1.0 mV to −67.6 ± 1.0 mV (Fig. 4 *a*). For intermediate concentrations of β3 cDNA (6–90 pg), both the individual (data not shown) and mean steady-state inactivation curves could be well fit only by a double Boltzmann function (Fig. 4 *a*). The two components of steady-state inactivation, A and B, had $V_{50,inact}$ values of ~−40 and −70 mV, respectively, which were relatively invariant (Fig. 4 *b*). However, the proportion of A decreased systematically, with a corresponding increase in B, as the amount of β3 cDNA, and therefore the concentration of expressed β3 protein, was increased (Fig. 4 *c*). On a log concentration plot, the percentage of A and B could be fit by reciprocal logistic functions with a midpoint of ~4 ng of β3 protein/oocyte (Fig. 4 *c*), corresponding to an average concentration of ~120 nM β3 protein.

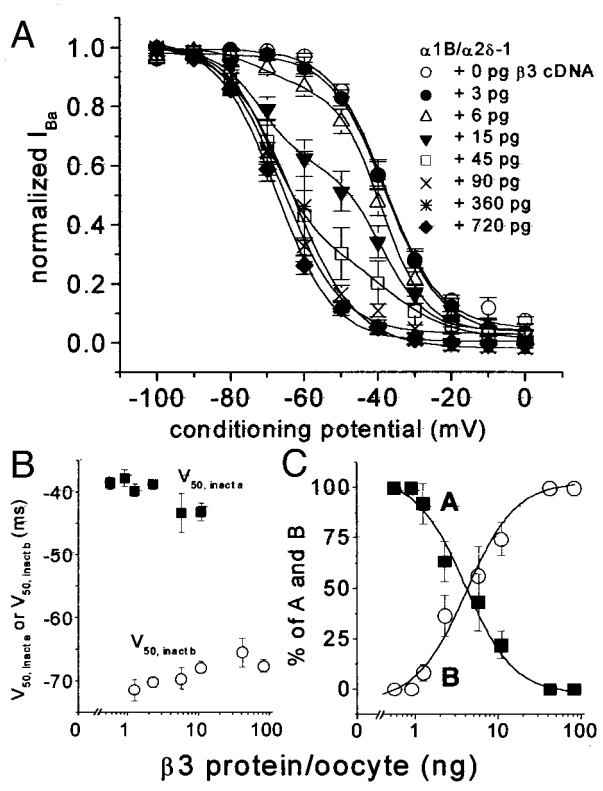

FIGURE 4 Effect of β3 subunit co-expression on steady-state inactivation of α1B. Steady-state inactivation curves were obtained from 100-ms-duration test pulses to 0 mV, preceded by a 25-s prepulse to the conditioning potential given (−100–0 mV). The fits are to a single or double Boltzmann function (see Materials and Methods). (*a*) Mean steady-state inactivation curves for α1B co-expressed with 0–720 pg of β3 cDNA. Peak I_{Ba} values from individual experiments were normalized and fit to either a single or a double Boltzmann function, as appropriate, judged by goodness-of-fit criteria. The symbols used are the same as in Fig. 2 *b*. (*b*) The mean values for $V_{50,inact,a}$ (■) and $V_{50,inact,b}$ (○) obtained for the two components of the individual steady-state inactivation curves, plotted against nanograms of β3 protein expressed, determined from Fig. 1 *b*, for each concentration of β3 cDNA injected (0–720 pg). (*c*) The mean percentage of the two components A (with $V_{50,inact,a}$) and B (with $V_{50,inact,b}$) from the individual normalized single or double Boltzmann fits are given for each concentration of β3 cDNA injected. The data are fit to logistic functions with midpoints at 4.25 and 4.43 ng of β3 protein and power coefficients (analogous to a Hill coefficient) of 1.28 and 1.20 for components A and B, respectively.

Dependence of the facilitation rate of G-protein-modulated α1B currents on β3 cDNA concentration

For the entire range of β3 cDNA injected, application of 100 nM quinpirole produced a significant inhibition of α1B I_{Ba}, being maximal between 64.4% and 73.1% (see traces in Fig. 5). This inhibition was voltage dependent, in that it could be overcome by a large depolarizing prepulse to +100 mV (voltage protocol in Fig. 5 *a*), a process termed facilitation. However, the duration of the prepulse required to overcome the inhibition was greater the lower the β-subunit concentration. The facilitation rate was studied by increasing the duration of the prepulse in successive sweeps (Fig. 5, *b–d*). Injection of the highest amount of the VDCC β3 cDNA (720 pg) caused a very marked increase in the facilitation rate of the G-protein-modulated I_{Ba} during a +100-mV prepulse, compared with that for the α1B/α2δ-1 currents in the absence of co-expressed β3-subunits (see example overlaid traces in Fig. 5 , *b* and *d*, and corresponding individual and mean facilitation rates in Fig. 5, *e* and *f*). At both these extremes, the individual and mean facilitation rates could be fit by a single exponential (Fig. 5, *e* and *f*). In the absence of co-expressed β3-subunits, the time constant for facilitation (τ_{facil}) was 94.7 ± 7.2 ms ($n = 12$; τ_{slow}). With 720 pg of β3 cDNA, τ_{facil} was 4.7 ± 0.4 ms ($n = 7$; τ_{fast}). We next examined whether the two extremes depicted in Fig. 5, *b* and *d*, represent facilitation of two separate populations, as suggested from the steady-state inactivation data. If this were the case, then injection of intermediate amounts of β3 cDNA would result in facilitation that could be fit by the sum of the two exponentials, represented by the extremes in Fig. 5, *e* and *f*. An example for an intermediate amount of β3 cDNA (45 pg) is given in Fig. 5 *c* (overlaid traces), and an example of the facilitation rate from an individual experiment is given in Fig. 5 *e* to show that it was well fit only by a double exponential. The double-exponential fits for each individual experiment at intermediate amounts of β3 cDNA resolved two components, A′ and B′, having time constants τ_{slow} and τ_{fast}. Their values, and their respective proportions, were determined from all the individual data whose mean facilitation curves are shown in Fig. 5 *f*. The percentage of A′ and B′ varied systematically and reciprocally with β3 cDNA injected, and therefore with concentration of β3 protein expressed (Fig. 5 *g*), in an almost identical manner to components A and B from the steady-state inactivation data (Fig. 4 *c*). The percentage of A′ and B′ could be fit with logistic functions, with half-maximal values at ~4 ng of β3 protein expressed/oocyte (Fig. 5 *g*).

Whereas the mean value of τ_{fast} was always similar to that observed with the maximal amount of injected β3 cDNA, being between 4.5 and 5.6 ms (Fig. 5 *h*, ○), the value of τ_{slow} was not constant but systematically decreased as the amount of β3 cDNA injected was increased, from over 90 ms in the absence of co-injected β3 cDNA to 27.0 ± 2.5 ms ($n = 10$) at 90 pg of injected β3 cDNA (Fig. 5 *h*, ■). The variation of τ_{slow} with the concentration of β3 protein expressed was fit by a logistic function, with a midpoint at 2.7 ng of β3 protein/oocyte. A plot of $1/\tau_{slow}$ versus β3 protein concentration is linear (Fig. 5 *h*, *inset*; $R = 0.9991$), with a slope of $6.9 \times 10^7\ M^{-1}\ s^{-1}$.

For the A/S ODN-injected oocytes, quinpirole-mediated voltage-dependent inhibition remained present, in those oocytes expressing I_{Ba}, with a very similar maximal degree of inhibition of I_{Ba} being observed for A/S and N/S ODN-injected oocytes (Fig. 6 *a*). The corresponding τ_{facil} was

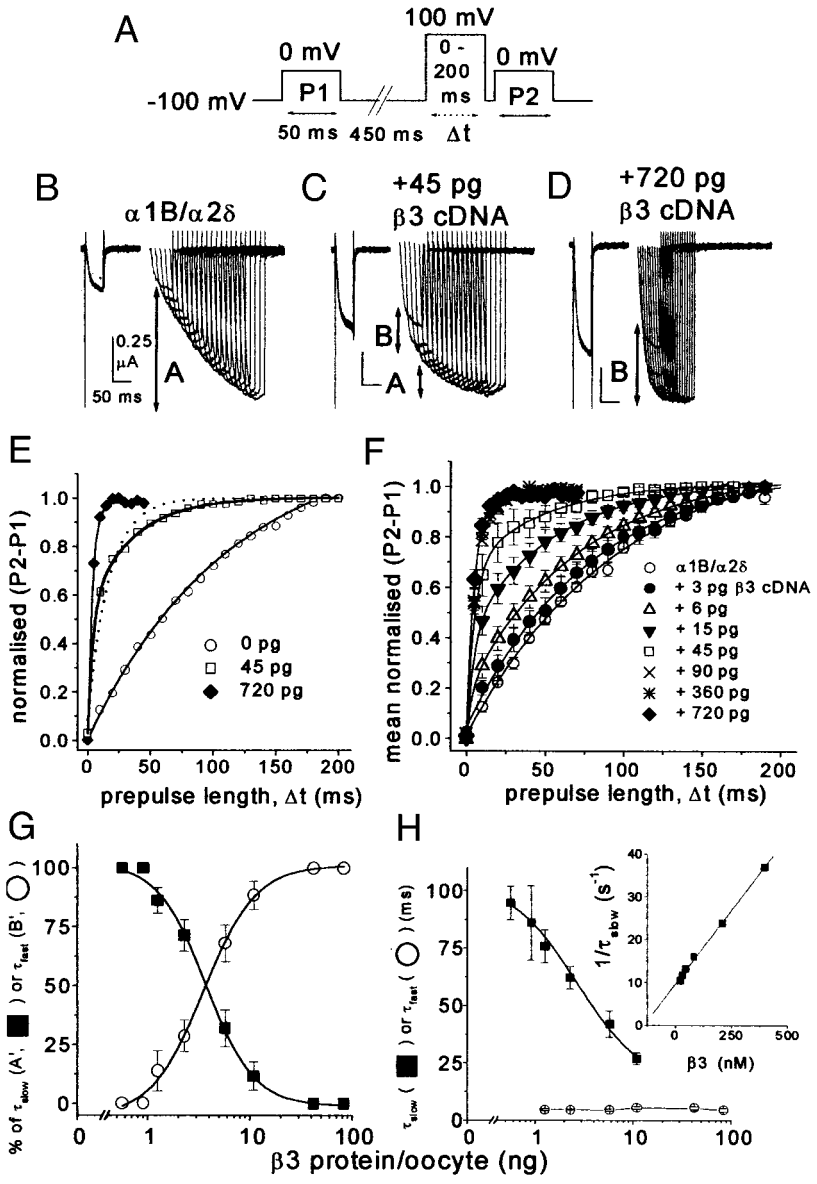

FIGURE 5 Effect of β3 subunit concentration on facilitation rates during inhibition of α1B currents by the dopamine D2 agonist quinpirole. (*a*) Voltage waveform for measurement of facilitation rate in the presence of quinpirole. The duration of the prepulse (Δt) was increased in 5- or 10-ms steps as appropriate for the time course. (*b–d*) Family of traces for the α1B/α2δ-1, α1B/α2δ-1 + 45 pg of β3 cDNA, and α1B/α2δ-1 + 720 pg of β3 cDNA subunit combinations. Tail currents have been clipped for better visualization of the currents. Calibrations in *b* refer to all traces. (*e*) Representative individual data for the facilitation rate are given for the intermediate concentration of 45 pg of β3 cDNA (□), compared with 0 pg of β3 cDNA (○) or 720 pg of β3 cDNA (◆), as used in *b–d* above. The difference between the amplitude of the P1 and P2 currents (P2-P1) at each Δt was normalized to the plateau (P2—P1) value and fit to a single- or double-exponential function. The 0- and 720-pg β3 cDNA facilitation rates are well fit by a single exponential (——; τ_{slow} = 106 ms, χ^2 = 0.00011 for the 0-pg β3 cDNA data; τ_{fast} = 3.72 ms, χ^2 = 0.00009), whereas the 45-pg β3 cDNA data are not well fit by a single exponential (· · ·; τ = 16.7 ms, χ^2 = 0.0187). In contrast, the points are well fit to a double exponential (——; τ_{fast} = 4.2 ms, 56%; τ_{slow} = 35.5 ms, 44%; χ^2 = 0.00011). (*f*) For the individual data at all β3 cDNA concentrations, the facilitation rates were determined as in *e*. The corresponding mean facilitation rates are shown, with single-exponential fits to the two β3 cDNA concentrations at each extreme (0 and 3 pg of β3 cDNA for τ_{slow} and 360 and 720 pg of β3 cDNA for τ_{fast}) and a double-exponential fit (τ_{slow} and τ_{fast}) for all the intermediate β3 cDNA concentrations. (*g*) The mean percentage of the two components A′ (■) and B′ (○) (with τ_{slow} and τ_{fast}, respectively), for the single- or double-exponential functions determined for the individual data, are given for each level of β3 protein expressed. The data are fit to logistic functions, both with midpoints of 3.7 ng of β3 protein expressed/oocyte and power coefficients 1.8 and 1.5, for components A′ and B′, respectively. (*h*) The values for τ_{slow} and τ_{fast} obtained for the two exponential components (A′ and B′) of the individual facilitation curves, for each concentration of β3 cDNA injected. The τ_{slow} data are fit with a logistic function with midpoint of 2.7 ng of β3 protein expressed/oocyte and power coefficient of 1.2. (*Inset*) Plot of $1/\tau_{slow}$ against estimated concentration of β3 protein expressed; slope (k_{slow}) = 6.86×10^7 M^{-1} s^{-1}.

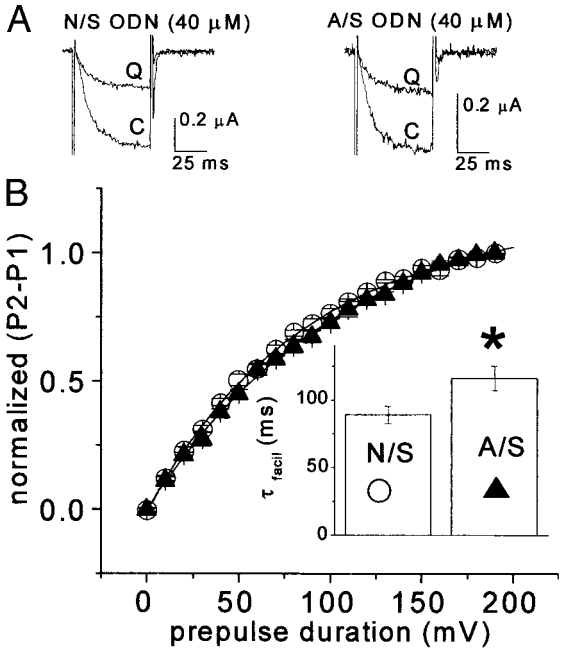

FIGURE 6 The effect of the β3 antisense ODN on kinetics of facilitation of α1B currents in the presence of quinpirole. (*a*) Examples of maximal inhibition of α1B I_{Ba} (*C*) by 100 nM quinpirole (*Q*) for 40 μM N/S and 40 μM A/S ODN injected oocytes. The test potential is −5mV. (*b*) Mean normalized facilitation time course (as in Fig. 5 *f*) for the N/S ODN and the combined 4 and 40 μM A/S ODN conditions in the presence of quinpirole, using the protocol in Fig. 5 *a*, both of which were fit to a single exponential. (*Inset*) Mean τ_{facil} (τ_{slow}) for the N/S and A/S conditions (n = 6 and 7, respectively). *$p < 0.05$, compared with the N/S ODN.

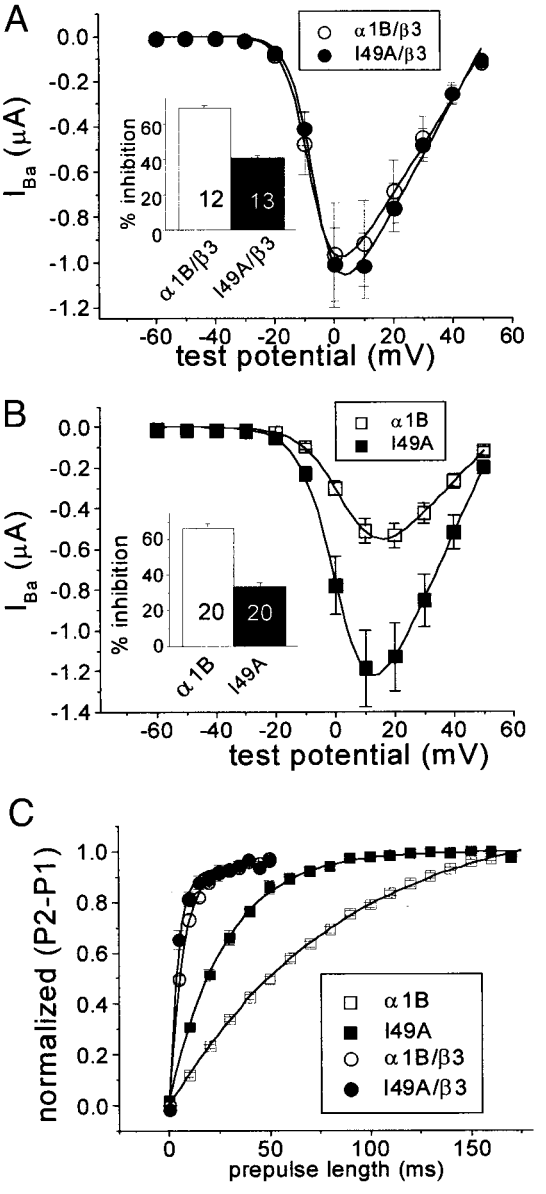

FIGURE 7 The effect of the I49A mutation of α1B on the expression and kinetics of facilitation of α1B currents in the absence and presence of co-expressed β3. (*a*) Mean *IV* relationships for α1B (○) and I49A α1B (●) I_{Ba} in the presence of a maximal concentration of co-expressed β3 (720 pg of β3 cDNA). (*Inset*) histogram of percent inhibition by 100 nM quinpirole at 0 mV, for the two conditions, with the n values given on the bars. (*b*) Mean *IV* relationships for α1B (□) and I49A α1B (■) I_{Ba} in the absence of co-expressed β3. (*Inset*) Histogram of percent inhibition by 100 nM quinpirole at 0 mV, for the two conditions, with the n values given on the bars. (*c*) Mean normalized facilitation time course (as in Fig. 5 *f*) for I_{Ba} in the presence of quinpirole, using the protocol in Fig. 5 *a* for the I49A (●, n = 13; ■, n = 20) and wild-type α1B (○, n = 12; □, n = 20), in the presence (○ and ●) or absence (□ and ■) of co-expressed β3 cDNA. Ba^{2+} (10 mM) was used as the charge carrier in these experiments. All time courses were fit to a single exponential, and mean data are given in the text.

~89 ms for currents in the N/S ODN-injected oocytes, almost identical to that obtained above for α1B/α2δ-1 expressed in the absence of exogenous β3 cDNA (Fig. 6, *b* and *inset*). τ_{facil} remained a single exponential but was significantly slower for I_{Ba} recorded from the β3 A/S ODN-injected oocytes, being ~116 ms for both 4 and 40 μM A/S ODN (Fig. 6, *b* and *inset*).

The effect of β3-subunit on the expression and facilitation rate of the N-terminal α1B mutant I49A

We have previously shown that the N-terminal amino acid sequence 45–55 of α1B contains critical determinants for Gβγ modulation and that mutation of I49 to A causes partial loss of G protein modulation (Canti et al., 1999), as confirmed here (Fig. 7, *a* and *b*, *insets*). We have subsequently shown that this motif is involved in VDCC β-subunit-regulated inactivation of α1B (Stephens et al., 2000). We have therefore compared the amount of expression and the facilitation rate of wild-type α1B with that of the I49A mutant of α1B, both in the absence and in the presence of co-injected β3 cDNA. In the presence of heterologously expressed β3-subunit, the expression of I49A mutant and wild-type α1B was identical, with the G_{max} values being 0.024 ± 0.003 (n = 13) and 0.022 ± 0.005 (n = 12) μS,

respectively (Fig. 7 *a*). In contrast, in the absence of co-expressed β3-subunit, the expression of I49A α1B was more than double that of the wild-type α1B, with the G_{max} values being 0.033 ± 0.004 ($n = 20$) and 0.015 ± 0.002 ($n = 20$) μS, respectively ($p < 0.01$; Fig. 7 *b*). This suggests the possibility that the I49A α1B has an increased affinity for the endogenous β3 responsible for trafficking it to the membrane. In agreement with this hypothesis, the facilitation rate for I49A α1B in the absence of co-expressed β3-subunit could be fit by a single exponential (Fig. 7 *c*), giving a τ_{facil} of 28.3 ± 1.7 ms ($n = 10$), which is nearly threefold faster than for wild-type α1B (84.3 ± 3.1 ms; $n = 9$; $p < 0.0001$; Fig. 7 *c*). For α1B I49A in the presence of a maximal concentration of β3-subunit protein (720 pg of β3 cDNA injected), the facilitation rate for this mutant was slightly faster (4.7 ± 0.5 ms; $n = 8$), than for wild-type α1B (7.4 ± 0.5 ms; $n = 5$; $p < 0.01$; Fig. 7 *c*). This small increase in the presence of β3 may represent an enhancement of the off-rate for Gβγ in the presence of β3, as suggested previously (Canti et al., 1999).

DISCUSSION

Effect of β3-subunit concentration on G_{max} of α1B currents

The endogenous oocyte concentration of β3 protein is here estimated to be ~17 nM, and the α1B G_{max} was strongly dependent on the concentration of heterologously expressed β3, with a half-maximal value at approximately the endogenous level of β3 protein. This correlates well with the affinity of the I-II linker of α1B for the β3-subunit, determined from Biacore experiments to be ~20 nM. This region has recently been suggested to harbor an endoplasmic reticulum retention signal, masked by a β-subunit (Bichet et al., 2000). We may therefore express this interaction as:

$$\alpha 1B + \beta 3 \overset{K_D \approx 17\ nM}{\rightleftharpoons} \alpha 1B \cdot \beta 3. \qquad (1)$$

Furthermore, the β3 A/S ODN reduced the number of cells expressing I_{Ba} and, in those oocytes that did express currents, reduced the mean G_{max} by ~50%. This is in close correlation with the estimated 47% reduction of endogenous β3 protein by the A/S ODN found in those cells expressing I_{Ba}. It also agrees with previous results on α1E expression, where it was suggested that the endogenous *Xenopus* oocyte β3-subunit plays an essential trafficking role (Tareilus et al., 1997). It was unclear from that study whether the endogenous chaperoning β3-subunits remain associated with each expressed α1-subunit in the plasma membrane in a high-affinity complex, because they do not affect the biophysical properties of the channel (Tareilus et al., 1997). Thus, the endogenous level of β3 protein appears to be insufficient to produce the effects of β-subunits on biophysical properties that are observed on heterologous expression of β-subunits. This is reinforced by the finding in the present study that there was no effect of partial depletion of the endogenous β-subunit by the A/S ODN on the $V_{50,act}$ of the residual I_{Ba}. In apparent contradiction to this, if the affinity for β3 remains at 17 nM, because the endogenous concentration of β3-subunit is estimated to be ~17 nM, when α1B is expressed alone it should be at least 50% bound in the membrane to a single endogenous β3-subunit via the I-II linker in the control or N/S ODN condition (to form α1B · β3; Eq. 1).

We can put forward two alternative hypotheses to account for the present results. Either a second β-subunit is bound, which accounts for the biophysical effects of β-subunits on the voltage dependence of activation and inactivation and on the facilitation rate, or there is a reduction in affinity of the mature α1B-subunit in the polarized plasma membrane for the β3-subunit responsible for its trafficking, so that the two species dissociate, and mature α1B-subunits are largely non-complexed to β-subunits at the endogenous level of *Xenopus* oocyte β-subunits. In agreement with either hypothesis, injection of β3 protein into *Xenopus* oocytes expressing α1C-subunits alone had acute effects on their biophysical properties (Yamaguchi et al., 1998), although the concentration dependence was not studied.

Effect of β-subunit concentration on voltage dependence of activation and steady-state inactivation

The effect of increasing the concentration of the β3-subunit on the $V_{50,act}$ revealed that the concentration dependence was right-shifted, compared with that for the G_{max}. However, we did not attempt in this study to resolve these data into two populations, as was done for the $V_{50,inact}$. The effect of increasing the concentration of the β3-subunit on the $V_{50,inact}$ fits the hypothesis that there are two populations of α1B channel, A and B, with independent behaviors, corresponding to α1B associated or not with a β-subunit, bound with the K_D of ~120 nM for β3. Both of the hypotheses outlined above are compatible with this result: either a second β-subunit is bound or the affinity of the β3-subunit for the mature α1B channel is markedly reduced, compared with its affinity for the nascent channel. Thus, population A would represent either α1B bound to a single β-subunit or free α1B in the plasma membrane (and for both cases, it is denoted α1B*). Population B would be α1B* · β3:

$$\underset{\text{(population A)}}{\alpha 1B^* + \beta 3} \overset{K_D \approx 120\ nM}{\rightleftharpoons} \underset{\text{(population B)}}{\alpha 1B^* \cdot \beta 3}. \qquad (2)$$

The equilibrium relationship between the populations A and B implies the presence of a pool of free β-subunits (Eq. 2), a notion that is supported by the fractionation experiment. Injection of 30 pg of β3 cDNA (producing ~120 nM β3 protein) results in an ~7-fold increase in β3 protein expres-

sion compared with the endogenous level and a proportionately greater increase in cytoplasmic β3. However, this results in only a 2-fold increase in the α1B G_{max}, again pointing to a large excess of β3-subunits over α1B channels.

Effect of VDCC β3-subunits on the facilitation rate of G-protein-modulated α1B

In the present experiments in *Xenopus* oocytes, which contain endogenous β3-subunits, G protein modulation via activation of the co-expressed dopamine D2 receptor was observed both in the absence and presence of heterologously expressed β3-subunits, as previously shown (Canti et al., 1999, 2000). In a previous study in COS-7 cells, we found that tonic voltage-dependent G protein modulation via co-expressed G$\beta\gamma$ dimers (as detected by its reversal by a depolarizing prepulse) was lost in the absence of co-expressed β-subunit (Meir et al., 2000). We were unable to detect any β-subunit protein in COS-7 cells by immunocytochemistry, although this does not exclude the expression of very low levels (Meir et al., 2000). We concluded from that study that β-subunits were essential for the process of facilitation, that is, the voltage-dependent removal of G$\beta\gamma$-subunits from the channel. In COS-7 cells, receptor-mediated inhibition via activation of the D2 dopamine receptor was not abolished in the absence of co-expressed β-subunits, but reversal of this inhibition by a 100-ms prepulse was lost (Meir et al., 2000). The main difference between the results obtained in COS-7 cells and those in *Xenopus* oocytes is that the endogenous level of β-subunits is substantial in oocytes, and in the antisense depletion experiments we were never able to abolish voltage-dependent receptor-mediated G protein modulation while retaining expression of α1B currents. This may point to the possible involvement of additional factors in this coupling process or that the complement of endogenous G$\beta\gamma$ dimers are different in *Xenopus* oocytes and mammalian cells.

The slow activation and facilitation of G-protein-modulated α1B calcium channels is thought to involve G$\beta\gamma$ unbinding from the channel, induced by depolarization, because re-inhibition following a prepulse is G$\beta\gamma$ concentration dependent (Stephens et al., 1998; Zamponi and Snutch, 1998). In the present experiments, the facilitation rate in the absence of injected β3 cDNA was 0.011 s^{-1} ($1/\tau_{slow}$) and was increased to 0.22 s^{-1} ($1/\tau_{fast}$) at the highest concentrations of β3 protein, in agreement with previous results (Roche and Treistman, 1998; Canti et al., 2000). However, at intermediate concentrations of β3-subunit, the facilitation rate could be fit only by the sum of two exponential components, with proportions almost identical to the two populations of channels defined by the steady-state inactivation data (compare Figs. 4 *c* and 5 *g*). This strongly supports the notion that A and B represent the same populations in the two experimental paradigms. Furthermore, τ_{fast} was relatively constant, at ~5 ms. It is likely that the population of channels termed B, with the invariant τ_{fast}, represents α1B* · β (Eq. 2). Thus, the facilitation rate exhibited by this population may approximate to the G$\beta\gamma$ dimer dissociation rate at +100 mV from this β-subunit-bound α1B species (Stephens et al., 1998), as follows:

$$\alpha 1B^* \cdot \beta 3 \cdot G\beta\gamma \rightleftharpoons \alpha 1B^* \cdot \beta 3 + G\beta\gamma. \qquad (3)$$

Does the β-subunit bind to α1B during a depolarizing prepulse?

From the facilitation data described above, we might conclude that the channel population termed A represents α1B* in this experimental paradigm, as also hypothesized for the steady-state inactivation experiments. However, τ_{facil} (τ_{slow}) is not invariant for this population but shows a marked decrease with increasing β3-subunit concentration and is also influenced in the opposite manner by A/S ODN treatment. We therefore hypothesize that the variation of the facilitation τ_{slow} with β3-subunit concentration reflects a depolarization-state-dependent increase in affinity of α1B* channels for β3-subunits, resulting in a disruption of the equilibrium described in Eq. 2. If a single β-subunit is bound during this process, the rate of β3 binding during the prepulse would vary linearly with β3 concentration (Fig. 5 *h*, *inset*) as follows:

$$\alpha 1B^* \cdot G\beta\gamma + \beta 3 \underset{+\Delta V}{\rightleftharpoons} \alpha 1B^* \cdot \beta 3 \cdot G\beta\gamma. \qquad (4)$$

Binding of β3 would be followed by rapid dissociation of G$\beta\gamma$ dimers at +100 mV, at the same rapid rate (0.22 s^{-1}) as observed for the α1B* channel population (B) to which β is already bound (Eq. 3).

During the +100-mV prepulse, the apparent increase in affinity for the β-subunit might also relate to the high affinity of the nascent channel for the β-subunit during the trafficking process (Eq. 1). The membrane potential difference across the endoplasmic reticulum is thought to be either zero or lumen-negative by analogy with the sarcoplasmic reticulum (Baylor et al., 1984).

If our hypothesis of additional β-subunit binding during facilitation is correct, from Fig. 5 *h* (*inset*) the specific k_{on} for β3 binding during the prepulse was calculated to be 6.9×10^7 M^{-1} s^{-1}, although this assumes a negligible off-rate during the period of measurement. There are, however, alternative hypotheses that could account for these data; for example, it may be possible to resolve the facilitation time courses into three exponentials, the slowest representing the G$\beta\gamma$ off-rate from free α1B, the next representing the G$\beta\gamma$ off-rate from α1B with one β-subunit bound, and the fastest representing the G$\beta\gamma$ off-rate from α1B with two β-subunits bound. This hypothesis would not require β-subunit binding during the prepulse and is a possibility that will be explored in the future.

How many β-subunits are bound to α1B?

The effect on the G_{max} of increasing the β3-subunit concentration occurs at a 7-fold lower concentration range of β3 protein than for the equilibrium between the populations A and B for the steady-state inactivation and facilitation data. This supports the hypothesis that there are two distinct binding processes for β-subunits on α1B. One explanation is that a single binding site undergoes a marked reduction in affinity for β-subunits once the α1-subunit is inserted in the polarized plasma membrane. Alternatively, we might postulate the co-existence of two separate β-subunit-binding sites on each α1B molecule, although some evidence argues against this hypothesis. The isolated I-II linker of α1 subunits has a high-affinity binding site for β-subunits (Pragnell et al., 1994; De Waard et al., 1995), and there are two other low-affinity sites on the N- and C-termini of various α1-subunits (Qin et al., 1997; Walker et al., 1998, 1999). However, none of the in vitro binding studies has addressed whether there is one complex binding pocket in an intact channel, such that the same β-subunit binds with high affinity to the I-II linker and with lower affinity to the N- and C-termini, or whether two different β-subunits can bind to a single channel.

A mutation in the I-II linker of α1A (Y392S) not only reduced the binding affinity for β-subunits in vitro and markedly lowered the expression of α1A currents but also prevented the β-subunit-induced hyperpolarization of current activation (Pragnell et al., 1994). Similar data have been obtained for other mutations in the I-II linker of α1A and α1E (Herlitze et al., 1997; Berrou et al., 2001). Here we report complementary data for the N-terminus of α1B, in which the I49A mutation not only affects the ability of β3 to influence the facilitation rate of α1B but also influences the G_{max}, both indicating an increased affinity for α1B. However, we have not found measurable binding of β3 to the isolated α1B N-terminus in the Biacore system (N.S.B. and A.C.D., unpublished results), suggesting that the N-terminal motif is a β-binding-site modifier rather than an independent binding site. This supports the interpretation of the present data that the differing concentration dependence of the effects of β3-subunits on trafficking and on biophysical properties of α1B do not depend on physically separate binding sites but rather on one complex binding site, whose affinity for β-subunits is high for the nascent calcium channel but is reduced once the channel has reached the polarized plasma membrane and is transiently enhanced by depolarization. This is also supported by purification studies reporting a 1:1 stoichiometry for α1- and β-subunits (Tanabe et al., 1987; Hosey et al., 1989; Witcher et al., 1993). Nevertheless, it still remains possible that the first β-subunit binds in the complex binding pocket outlined above, and the second β-subunit subsequently binds largely via interaction with the first β-subunit. In this regard we have recently identified that β-subunits have a domain structure reminiscent of the membrane-associated guanylate kinase (MAGUK) family (Hanlon et al., 1999), and such proteins may form intermolecular interactions within subfamilies (Wu et al., 2000).

The hypothesis proposed here that at a physiological membrane potential β3-subunits are in equilibrium with the α1B subunits is not at odds with a 1:1 stoichiometry in the channel complex, because under most native conditions, as with our standard cDNA injection conditions (Canti et al., 2000), it may well be that there is a sufficient excess of β-subunit that almost all α1 subunits are associated with a bound β-subunit. It remains to be determined whether this is the case for native calcium channels. Furthermore, during the purification process of the α1 subunit, the potential difference across the channel, and its native conformation, would rapidly be lost, and the affinity of β-subunits for the channels might thus be enhanced. These hypotheses will be investigated in a future study. We shall also consider in the future the role of the C-terminus of α1B in forming part of, or modifying, a complex binding site for the β-subunits, because there is much evidence for the C-terminus of other calcium channels playing a part in this process (Walker et al., 1998).

We thank Dr. S. Volsen, Eli Lilly Research UK, for the gift of the β3 monoclonal antibody. We acknowledge financial support from The Wellcome Trust, Medical Research Council, and the European Community (Marie Curie Fellowship to C.C.). We are grateful to Dr. Alon Meir for advice and discussion.

REFERENCES

Baylor, S. M., W. K. Chandler, and M. W. Marshall. 1984. Calcium release and sarcoplasmic reticulum membrane potential in frog skeletal muscle fibres. *J. Physiol. (Lond.).* 348:209–238.

Bell, D. C., A. J. Butcher, N. S. Berrow, K. M. Page, P. F. Brust, A. Nesterova, K. A. Stauderman, G. R. Seabrook, B. Nürnberg, and A. C. Dolphin. 2001. Biophysical properties, pharmacology and modulation of human, neuronal L-type (α1D, $Ca_V1.3$) voltage-dependent calcium currents. *J. Neurophysiol.* 85:816–828.

Berrou, L., G. Bernatchez, and L. Parent. 2001. Molecular determinants of inactivation within the I-II linker of α1E ($Ca_V2.3$) calcium channels. *Biophys. J.* 80:215–228.

Bichet, D., V. Cornet, S. Geib, E. Carlier, S. Volsen, T. Hoshi, Y. Mori, and M. De Waard. 2000. The I-II loop of the Ca^{2+} channel alpha(1) subunit contains an endoplasmic reticulum retention signal antagonized by the beta subunit. *Neuron.* 25:177–190.

Birnbaumer, L., N. Qin, R. Olcese, E. Tareilus, D. Platano, J. Costantin, and E. Stefani. 1998. Structures and functions of calcium channel β-subunits. *J. Bioenerg. Biomembr.* 30:357–375.

Bogdanov, Y., N. L. Brice, C. Canti, K. M. Page, M. Li, S. G. Volsen, and A. C. Dolphin. 2000. Acidic motif responsible for plasma membrane association of the voltage-dependent calcium channel β1b subunit. *Eur. J. Neurosci.* 12:894–902.

Bourinet, E., T. W. Soong, A. Stea, and T. P. Snutch. 1996. Determinants of the G protein-dependent opioid modulation of neuronal calcium channels. *Proc. Natl. Acad. Sci. U.S.A.* 93:1486–1491.

Brabet, P., C. Pantaloni, B. Rouot, M. Toutant, A. Garcia-Sainz, J. Bockaert, and V. Homburger. 1988. Multiple species and isoforms of *Bordetella pertussis* toxin substrates. *Biochem. Biophys. Res. Commun.* 152:1185–1192.

Brice, N. L., N. S. Berrow, V. Campbell, K. M. Page, K. Brickley, I. Tedder, and A. C. Dolphin. 1997. Importance of the different β subunits in the membrane expression of the α1A and α2 calcium channel subunits: studies using a depolarisation-sensitive α1A antibody. *Eur. J. Neurosci.* 9:749–759.

Burgess, D. L., G. H. Biddlecome, S. I. McDonough, M. E. Diaz, C. A. Zilinski, B. P. Bean, K. P. Campbell, and J. L. Noebels. 1999. β Subunit reshuffling modifies N- and P/Q-type Ca^{2+} channel subunit compositions in lethargic mouse brain. *Mol. Cell. Neurosci.* 13:293–311.

Campbell, V., N. Berrow, K. Brickley, K. Page, R. Wade, and A. C. Dolphin. 1995. Voltage-dependent calcium channel β-subunits in combination with alpha1 subunits have a GTPase activating effect to pro mote hydrolysis of GTP by G $alpha_o$ in rat frontal cortex. *FEBS Lett.* 370:135–140.

Campbell, V., N. S. Berrow, E. M. Fitzgerald, K. Brickley, and A. C. Dolphin. 1995. Inhibition of the interaction of G protein G_o with calcium channels by the calcium channel β-subunit in rat neurones. *J. Physiol. (Lond.).* 485:365–372.

Canti, C., Y. Bogdanov, and A. C. Dolphin. 2000. Interaction between G proteins and accessory β subunits in the regulation of α1B calcium channels in *Xenopus* oocytes. *J. Physiol. (Lond.).* 527:419–432.

Canti, C., K. M. Page, G. J. Stephens, and A. C. Dolphin. 1999. Identification of residues in the N-terminus of α1B critical for inhibition of the voltage-dependent calcium channel by Gβγ. *J. Neurosci.* 19: 6855–6864.

Day, N. C., S. G. Volsen, A. L. McCormack, P. J. Craig, W. Smith, R. E. Beattie, P. J. Shaw, S. B. Ellis, M. M. Harpold, and P. G. Ince. 1998. The expression of voltage-dependent calcium channel beta subunits in human hippocampus. *Mol. Brain Res.* 60:259–269.

De Waard, M., and K. P. Campbell. 1995. Subunit regulation of the neuronal α_{1A} Ca^{2+} channel expressed in *Xenopus* oocytes. *J. Physiol. (Lond.).* 485:619–634.

De Waard, M., H. Y. Liu, D. Walker, V. E. S. Scott, C. A. Gurnett, and K. P. Campbell. 1997. Direct binding of G-protein βgamma complex to voltage-dependent calcium channels. *Nature.* 385:446–450.

De Waard, M., D. R. Witcher, M. Pragnell, H. Liu, and K. P. Campbell. 2064. 1995. Properties of the α_1-β anchoring site in voltage-dependent Ca^{2+} channels. *J. Biol. Chem.* 270:12056–12061.

Dolphin, A. C. 1998. Mechanisms of modulation of voltage-dependent calcium channels by G proteins. *J. Physiol. (Lond.).* 506:3–11.

Hanlon, M. R., N. S. Berrow, A. C. Dolphin, and B. A. Wallace. 1999. Modelling of a voltage-dependent Ca^{2+} channel β subunit as a basis for understanding its functional properties. *FEBS Lett.* 445:366–370.

Herlitze, S., G. H. Hockerman, T. Scheuer, and W. A. Catterall. 1997. Molecular determinants of inactivation and G protein modulation in the intracellular loop connecting domains I and II of the calcium channel α_{1A} subunit. *Proc. Natl. Acad. Sci. U.S.A.* 94:1512–1516.

Hosey, M. M., F. C. Chang, C. M. O'Callahan, and J. Ptasienski. 1989. L-type calcium channels in cardiac and skeletal muscle: purification and phosphorylation. *Ann. NY Acad. Sci.* 560:27–38.

Meir, A., D. C. Bell, G. J. Stephens, K. M. Page, and A. C. Dolphin. 2000. Calcium channel β subunit promotes voltage-dependent modulation of α1B by Gβγ. *Biophys. J.* 79:731–746.

Pragnell, M., M. De Waard, Y. Mori, T. Tanabe, T. P. Snutch, and K. P. Campbell. 1994. Calcium channel β-subunit binds to a conserved motif in the I-II cytoplasmic linker of the α_1-subunit. *Nature.* 368:67–70.

Qin, N., D. Platano, R. Olcese, E. Stefani, and L. Birnbaumer. 1997. Direct interaction of Gβgamma with a C terminal Gβgamma binding domain of the calcium channel α1 subunit is responsible for channel inhibition by G protein coupled receptors. *Proc. Natl. Acad. Sci. U.S.A.* 94: 8866–8871.

Roche, J. P., and S. N. Treistman. 1998. The calcium channel β3 subunit enhances voltage-dependent relief of G protein inhibition induced by muscarinic receptor activation and Gβgamma. *J. Neurosci.* 18: 4883–4890.

Stephens, G. J., N. L. Brice, N. S. Berrow, and A. C. Dolphin. 1998. Facilitation of rabbit α1B calcium channels: involvement of endogenous Gβgamma subunits. *J. Physiol. (Lond.).* 509:15–27.

Stephens, G. J., K. M. Page, Y. Bogdanov, and A. C. Dolphin. 2000. The α1B calcium channel amino terminus contributes determinants for β subunit mediated voltage-dependent inactivation properties. *J. Physiol. (Lond.).* 525:377–390.

Stephens, G. J., K. M. Page, J. R. Burley, N. S. Berrow, and A. C. Dolphin. 1997. Functional expression of rat brain cloned α1E calcium channels in COS-7 cells. *Pflügers Arch.* 433:523–532.

Tanabe, T., H. Takeshima, A. Mikami, V. Flockerzi, H. Takahashi, K. Kangawa, M. Kojima, H. Matsuo, T. Hirose, and S. Numa. 1987. Primary structure of the receptor for calcium channel blockers from skeletal muscle. *Nature.* 328:313–318.

Tareilus, E., M. Roux, N. Qin, R. Olcese, J. M. Zhou, E. Stefani, and L. Birnbaumer. 1997. A *Xenopus* oocyte β subunit: evidence for a role in the assembly/expression of voltage-gated calcium channels that is separate from its role as a regulatory subunit. *Proc. Natl. Acad. Sci. U.S.A.* 94:1703–1708.

Walker, D., D. Bichet, K. P. Campbell, and M. De Waard. 1998. A β_4 isoform-specific interaction site in the carboxyl-terminal region of the voltage-dependent Ca^{2+} channel α_{1A} subunit. *J. Biol. Chem.* 273: 2361–2367.

Walker, D., D. Bichet, S. Geib, E. Mori, V. Cornet, T. P. Snutch, Y. Mori, and M. De Waard. 1999. A new β subtype-specific interaction in α1A subunit controls P/Q type Ca^{2+} channel activation. *J. Biol. Chem.* 274:12383–12390.

Witcher, D. R., M. De Waard, J. Sakamoto, C. Franzini-Armstrong, M. Pragnell, S. D. Kahl, and K. P. Campbell. 1993. Subunit identification and reconstitution of the N-type Ca^{2+} channel complex purified from brain. *Science.* 261:486–489.

Wu, H., C. Reissner, S. Kuhlendahl, B. Coblentz, S. Reuver, S. Kindler, E. D. Gundelfinger, and C. C. Garner. 2000. Intramolecular interactions regulate SAP97 binding to GKAP. *EMBO J.* 19:5740–5751.

Yamaguchi, H., M. Hara, M. Strobeck, K. Fukasawa, A. Schwartz, and G. Varadi. 1998. Multiple modulation pathways of calcium channel activity by a β subunit - Direct evidence of β subunit participation in membrane trafficking of the α_{1c} subunit. *J. Biol. Chem.* 273:19348–19356.

Zamponi, G. W., E. Bourinet, D. Nelson, J. Nargeot, and T. P. Snutch. 1997. Crosstalk between G proteins and protein kinase C mediated by the calcium channel α_1 subunit. *Nature.* 385:442–446.

Zamponi, G. W., and T. P. Snutch. 1998. Decay of prepulse facilitation of N type calcium channels during G protein inhibition is consistent with binding of a single $G_{\beta gamma}$ subunit. *Proc. Natl. Acad. Sci. U.S.A.* 95:4035–4039.